

A multi-reference coupled-cluster study on the potential energy surface of N₂ including ground and excited states: spin projections and wavefunction overlaps

Michael Hanrath · Anna Engels-Putzka

Received: 17 October 2008 / Accepted: 9 December 2008 / Published online: 27 December 2008
© Springer-Verlag 2008

Abstract This article reports on the calculation of 12 low lying states of the nitrogen molecule along its dissociation using the multi-reference exponential wavefunction ansatz (Hanrath in J Chem Phys 123:84102, 2005), the single-reference formalism multi-reference coupled cluster (Oliphant and Adamowicz in J Chem Phys 94:1229, 1991), and MRCI methods. Spin projection errors and state overlap errors are calculated and allow an analysis of the wavefunction with respect to properties different from correlation energies. Both criteria are very sensitive to errors in the wavefunction. Due to its lack of Fermi vacuum invariance the errors are more significant for the single-reference formalism based approach.

Keyword Coupled-cluster · Multi-reference · State selective · Electronic structure · MRCC

1 Introduction

The triple bond breaking of the N₂ molecule is one of the most difficult problems of quantum chemistry. Due to the difficulties in the generalization of single-reference coupled cluster (SRCC) methods [1, 2] to the multi-reference case (MRCC), calculations on N₂ involving the bond breaking were dominated by MRCI and CASPT2 [3–5] methods in the past. N₂ is of particular interest as a proper description has to meet several criteria which would be best fulfilled with some kind of MRCC method. N₂ offers a geometry depending and partially significant amount of

static (near degeneracy) and dynamic (electron cusp) correlation at the same time and offers several qualitative symmetry related properties that should be met rigorously by approximative calculations.

The MRCC history starts back in 1975 with the work of Mukherjee et al. [6] and later [7] on valence universal or Fock space coupled cluster (FSMRCC) theory. Lindgren [8] as well as Lindgren and Mukherjee [9] and Mukherjee and Pal [10] continued to work on FSMRCC. Another branch of the MRCC history is started by the introduction of the Hilbert space or state universal (SUMRCC) approach of Jeziorski and Monkhorst in 1981 [11]. Both, FSMRCC and SUMRCC, branches employ the Bloch equation and suffer (in their original formulation) from various limitations. For a more elaborate discussion of these branches we refer to [12–15].

Besides the state and valence *universal* methods the development started on state *specific* approaches. These may be divided into single reference formalism based and real multi-reference approaches. Naturally, the single reference formalism based multi-reference coupled cluster (SRMRCC) approach of Oliphant and Adamowicz [16] belongs to the former category. Li and Paldus introduced reduced MRCC [17] and partially linearized reduced MRCC approaches [18, 19] which are also formally based on a single reference ansatz. Although there are many advantages of these approaches they share the problem of symmetry breaking as they treat one reference particular.

Apart from the single reference formalism based approaches there are a few state specific variants of the SUMRCC approach: 1. The ansatz by Mahapatra et al. [20, 21] (MkMRCC), 2. Brillouin–Wigner based ansätze [22–25] (BWMRCC) from the groups of Hubac and Pittner, and 3. the multi-reference exponential (MRexpT) [26, 27] ansatz by one of the present authors. The

M. Hanrath (✉) · A. Engels-Putzka
Institute for Theoretical Chemistry, University of Cologne,
Greinstraße 4, 50939 Cologne, Germany
e-mail: Michael.Hanrath@uni-koeln.de

performance of those approaches has been analyzed in various publications [14, 15, 28, 29].

The goal of this paper is to study state overlap and spin projection errors for the SRMRCC and MRexpT wavefunction approaches in comparison to spin orbital oriented MRCI (SOMRCI). These properties are more sensitive to the quality of the wavefunction than the usually reported correlation energies.

This paper is organized as follows: in Sect. 2 we recapitulate the concepts of CI, MRCI, SRMRCC, and MRexpT with a certain focus on the difficulties related to MRCC. Section 3 reports the results of the calculations with Sects. 3.2 and 3.3 going into state overlap and spin projection errors, respectively.

2 Methods

In order to illustrate and describe the concepts of the MRCC approaches we briefly look into the ideas of CI and MRCI. The notation introduced during the discussion of the CI methods will allow us to formulate the MRCC approaches concisely.

2.1 CI

The CI wavefunction reads

$$|\Psi_{\text{CI}}\rangle = c_{\mu_0}|\mu_0\rangle + \sum_{\alpha \in \mathbb{Q}} c_{\alpha}|\alpha\rangle \quad (1)$$

with $|\mu_0\rangle$ the Hartree-Fock determinant and \mathbb{Q} a set of suitably chosen determinants. Individual CI (e.g. CIS, CISD, CISDT, etc.) variants just differ in the choice of a particular \mathbb{Q} . Starting from a dominant Hartree-Fock determinant μ_0 we may classify a certain determinant by its substitution level with respect to μ_0 . Considering the Hamilton matrix elements, the importance of a determinant α is (partially) ruled by the difference of the diagonal elements $\langle \mu_0 | \hat{H} | \mu_0 \rangle - \langle \alpha | \hat{H} | \alpha \rangle$. Since this difference typically grows with the substitution level one usually succeedingly includes all singles, doubles, or higher level substitutions in that order to improve the accuracy. Defining

$$\mathbb{Q}_x(\mu) = \bigcup_{\hat{\tau} \in \mathbb{T}_x(\mu)} \hat{\tau}|\mu\rangle \quad (2)$$

with $\mathbb{T}_x(\mu)$ all x -fold substitutions with respect to μ_0 we may simply write $\mathbb{Q}_{\text{CIS}} = \mathbb{Q}_S(\mu_0)$, $\mathbb{Q}_{\text{CISD}} = \mathbb{Q}_{SD}(\mu_0)$, etc.

2.2 MRCI

In case of degeneracy the Hartree-Fock determinant is no longer a good approximation of a desired state and we have

to include additional determinants in a so called “reference space” $\mathbb{P} = \{\mu_1, \mu_2, \dots\}$. The MRCI wavefunction reads

$$|\Psi_{\text{MRCI}}\rangle = \sum_{\mu \in \mathbb{P}} c_{\mu}|\mu\rangle + \sum_{\alpha \in \mathbb{Q}} c_{\alpha}|\alpha\rangle. \quad (3)$$

It remains to define \mathbb{Q} . As the above arguments regarding the importance of the substitution levels hold in the multi-reference case as well we should choose \mathbb{Q} accordingly. Obviously, in order to conserve the symmetry of the wavefunction with respect to its references we have to apply the same substitution level to each individual reference determinant.

This is illustrated in Fig. 1 for a singles substitution manifold. The square shaped vertices on the left hand side and the dots on the right hand side of the graph depict the references and the substituted determinants, respectively, while the arcs picture the substitution process. Considering the illustration given in Fig. 1 we see the determinant $|ia\rangle$ to be generated from the substitution $p \rightarrow a$ applied to $|ip\rangle$ and from the substitution $q \rightarrow a$ applied to $|iq\rangle$. In order to avoid $|ia\rangle$ occurring in the wavefunction twice (causing linear dependencies) we have to treat the collection of all substituted determinants as a set with every element occurring only once. Consequently, it is $\mathbb{Q}_{\text{MRCIS}} = \bigcup_{\mu \in \mathbb{P}} \mathbb{Q}_S(\mu) \setminus \mathbb{P}$, $\mathbb{Q}_{\text{MRCISD}} = \bigcup_{\mu \in \mathbb{P}} \mathbb{Q}_{SD}(\mu) \setminus \mathbb{P}$, etc., where we excluded \mathbb{P} from \mathbb{Q}_{\dots} to guarantee $\mathbb{P} \cap \mathbb{Q}_{\dots} = \emptyset$.

We should note that the discrimination of the \mathbb{P} and \mathbb{Q} space in the (MR)CI wavefunction Eq. 3 is artificial. Equivalently one may write

$$|\Psi_{\text{MRCI}}\rangle = \sum_{\rho \in \mathbb{A}_{\text{MRCI}}} c_{\rho}|\rho\rangle \quad (4)$$

with

$$\mathbb{A}_{\text{MRCI}} = \mathbb{P} \cup \bigcup_{\mu \in \mathbb{P}} \mathbb{Q}_x(\mu).$$

The equivalence between \mathbb{P} and \mathbb{Q} space with respect to their role in the wavefunction is no longer true for coupled cluster methods.

MRCI is a very general and accurate method with a single but very serious issue: MRCI is neither size

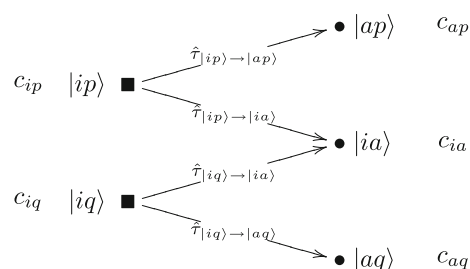


Fig. 1 Illustration of the MRCI wavefunction: linear ansatz \Rightarrow every generated linearly independent determinant carries its own coefficient

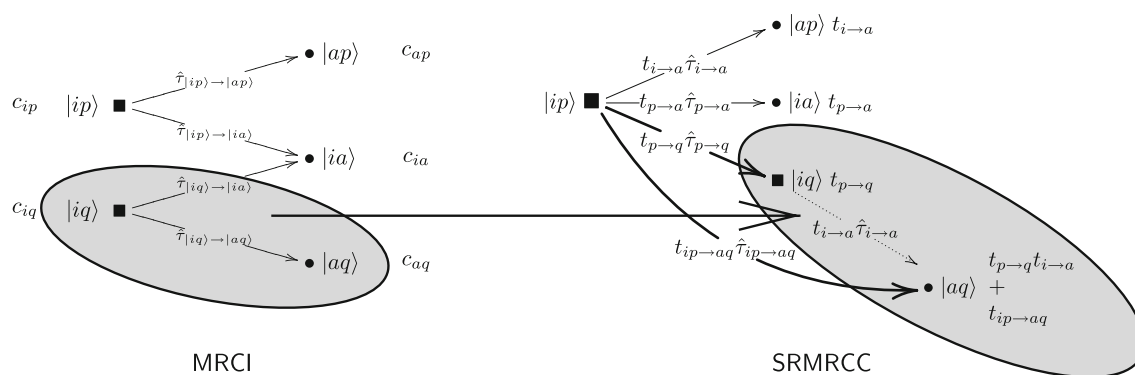


Fig. 2 Illustration of the SRMRCC wavefunction (including only the $\hat{\tau}_{p \rightarrow q} \hat{\tau}_{i \rightarrow a}$ product substitution for convenience) and its symmetry breaking, *left* original MRCI wavefunction, *right* inclusion of second

reference determinant $|iq\rangle$ and substitutions from it as (higher) excitations from a particular reference $|ip\rangle$ within the SRMRCC approach

consistent [30] nor size extensive [31]. This deficiency severely affects the accuracy when going to a larger number of particles.

2.3 SRMRCC

In 1991 Oliphant and Adamowicz [16] introduced an ansatz they called “multi-reference coupled-cluster method using a single-reference formalism” (SRMRCC). Using the notation of the previous subsections this approach may be written in a very concise form:

$$|\Psi_{\text{SRMRCC}}\rangle = e^{\hat{T}} |\mu_0\rangle \quad (5)$$

with $|\mu_0\rangle$ the Fermi vacuum and \hat{T} chosen to span the MRCI space according to

$$\hat{T} = \sum_{\hat{\tau} \in \Delta(\mathbb{A} \setminus \mu_0, \mu_0)} t_{\hat{\tau}} \hat{\tau} \quad (6)$$

with $\mathbb{A} = \mathbb{A}_{\text{MRCI}}$ and $\Delta(\alpha, \mu)$ returning the substitution from μ to α . Of course one may choose \mathbb{A} different from \mathbb{A}_{MRCI} in Eq. 6. However, according to the success of the MRCI method the original intention of [16] was to choose it as $\mathbb{A} = \mathbb{A}_{\text{MRCI}}$. Actually, for the latter choice SRMRCC is equivalent to an MRCI wavefunction (provided $c_{\mu_0} \neq 0$) upon linearization of the Taylor series of the exponential in Eq. 5 ($e^{\hat{T}} \sim 1 + \hat{T}$).

Figure 2 shows an illustration of the assembly of the SRMRCC wavefunction at singles substitution level including only the $\hat{\tau}_{p \rightarrow q} \hat{\tau}_{i \rightarrow a}$ product substitution. The left hand side of Fig. 2 shows an MRCI wavefunction similar to Fig. 1. Now we choose arbitrarily reference $|ip\rangle$ to act as Fermi vacuum. Considering the determinants generated from $|ip\rangle$ we find $|ap\rangle$ and $|ia\rangle$. Obviously $|iq\rangle$ and $|aq\rangle$ are missing and in order to assemble the original MRCI wavefunction one has to add them as (higher) excitations relative to $|ip\rangle$. This is depicted in Fig. 2 by the movement of the grayed area from the left to the right. On the right hand side

of Fig. 2 the additional substitutions are drawn as bold arrows. (Actually, in this simple example the other reference $|iq\rangle$ would be covered by a singles substitution manifold already. But attention: This is not to be generalized.)

Analyzing the coefficients of the determinants on the right hand side of Fig. 2 we find the coefficient of $|ap\rangle$ to be $t_{i \rightarrow a}$ while the coefficient of (the completely equivalent) $|aq\rangle$ is $t_{p \rightarrow q} t_{i \rightarrow a} + t_{ip \rightarrow aq}$ since $|aq\rangle$ may be additionally reached by a product excitation $\hat{\tau}_{i \rightarrow a}$ (the dotted arrow) from $|iq\rangle$. As $t_{p \rightarrow q}$ and $t_{i \rightarrow a}$ already appear in the graph they are not independent and cause the symmetry of the SRMRCC wavefunction to break.

Due to the previous discussion we may interpret SRMRCC as a plain single reference coupled cluster ansatz (e.g. CCSD) with additional specific higher excitations added. Alternatively it may be viewed as a single reference CCSDT... with certain excitations missing.

Without changing the original intention of [16] the SRMRCC ansatz was later generalized to more than two references [32] while keeping still only two electrons active. Later variants of the SRMRCC ansatz [33–36] do not solve the fundamental problem of symmetry breaking. Although usually of reasonable accuracy in terms of the correlation energy when using the dominant determinant as Fermi vacuum, SRMRCC has been shown to have difficulties in case of avoided crossings [28, 37], potential energy surfaces, and low-spin/high-spin degeneracies [26, 37]. Due to the similar wavefunction ansatz within RMRCC [17] and pl-RMRCC [18, 19] there are analogous symmetry issues with those approaches.

2.4 Conceptual difficulties upon generalizing SRCC or transferring MRCI to MRCC

One of the crucial points of the coupled cluster wavefunction is to contain products of (substitution, amplitude) pairs. This plays an important role for the wavefunction to be size

consistent and the cluster operator to be irreducible (connected) insuring size extensivity. In order to understand the difficulties of MRCC we shall try to reformulate CI and MRCI in terms of excitation operators. We shall see that the difficulties arise already at linear level and are not specific to the product terms generated by the exponential. The crucial problem is that an MRCI space cannot be spanned unambiguously by substitution operators as illustrated by Fig. 1.

Upon inspection of the CI and MRCI wavefunctions (Eqs. 1, 3) we find no explicit reference to excitations. However, we now rewrite the CI and MRCI wavefunctions in terms of excitations. Equation 1 written in terms of excitations reads

$$|\Psi_{\text{CI}}\rangle = c_{\mu_0}|\mu_0\rangle + \sum_{\hat{\tau} \in \mathbb{T}} t_{\hat{\tau}} \hat{\tau} |\mu_0\rangle. \quad (7)$$

Eq. 7 is completely equivalent to Eq. 1.

However, considering the multi-reference case there is no unique reformulation of Eq. 3 based on an excitation based picture. The problems arise due to the ambiguity of the excitation paths (e.g. $\hat{\tau}_{p \rightarrow a}|ip\rangle = \hat{\tau}_{q \rightarrow a}|iq\rangle$). In case of MRCI this problem was solved by the application of a set unification according to $\mathbb{Q}_{\text{MRCI}} = \bigcup_{\mu} \mathbb{Q}(\mu)$. Since the unification is applied to determinants it insures the linear independence of the MRCI function space. Obviously, in order for the set unification scheme to work it has to be applied globally to all determinants generated by substitutions from all references. However, this is a contradiction to the fact that the excitation manifolds are reference specific (that is: non-global). This prohibits the existence of a substitution based analogon to the MRCI scheme.

The MRexpT ansatz [26] was inspired by the following simple observation: If we cannot prohibit the existence of ambiguous substitution paths we have to address the problem of linear independence by the amplitudes. It has been shown [26] that a determinant based amplitude index insures linear independence.

We note that due to the single reference nature of the SRMRCC approach there is no ambiguity issue with it.

2.5 MRexpT

Similarly to SRMRCC the initial concept of MRexpT is very simple. The MRexpT ansatz [26, 27] is a state selective modification of the SUMRCC of Jeziorski and Monkhorst [11]. The MRexpT wavefunction is given by

$$|\Psi\rangle = \sum_{\mu} e^{\hat{T}_{\mu}} c_{\mu} |\mu\rangle \quad (8)$$

with

$$\hat{T}_{\mu} = \phi(c_{\mu}) \sum_{\hat{\tau}_{\mu,i} \in \mathbb{T}_{\mu}} t_{\hat{\tau}_{\mu,i}|\mu} \hat{\tau}_{\mu,i}. \quad (9)$$

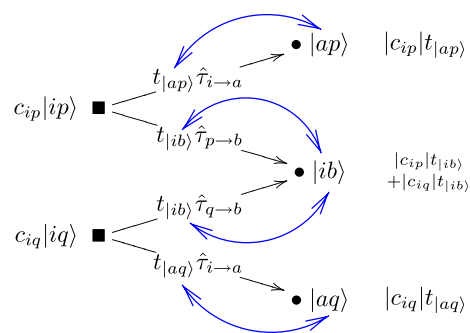


Fig. 3 Illustration of the MRexpT wavefunction: amplitudes leading to the same determinant share the same value

with \mathbb{T}_{μ} the set of substitutions to be applied (e.g. singles and doubles) with respect to each reference $|\mu\rangle$ while excluding excitations from one reference to another and $\phi(z) = e^{-i \arg z}$, $z \in \mathbb{C}$.

The major difference between the SUMRCC and the MRexpT ansatz is the way the amplitudes are indexed. The original SUMRCC ansatz used an excitation based indexing ($t_{\hat{\tau}_{\mu,i}|\mu}$) introducing many more variables into the wavefunction than may be fixed by projections (when considering a single state). Due to the determinant based indexing of the amplitudes ($t_{\hat{\tau}_{\mu,i}|\mu}$) this problem is avoided in MRexpT as illustrated in Fig. 3. The amplitudes are fixed (at linear level) by the target determinant they are pointing to. The wavefunction genealogy for MRexpT including product excitations is shown elsewhere [38].

However, there is a price one has to pay: As shown in [38] the coupling of the amplitudes leading to the same substituted determinants destroys core-valence connectivity. However, the core (=inactive) part remains connected. Additionally, MRexpT has been shown to be size consistent [26]. Finally, we note that upon linearization of the Taylor series of the exponential with suitably chosen \mathbb{T}_{μ} s also MRexpT is equivalent to MRCI.

Summarizing, each of the two discussed MRCC approaches has its own issues: SRMRCC is inherently symmetry broken while MRexpT lacks core-valence connectivity. However, we would like to point out that we are not aware of any MRCC approach up to now having no issues.

3 Results and discussion

In this section we present results for state overlaps and spin projection errors.

3.1 Calculation details

In accordance with [39], which reports on the correlation energies of N_2 for MRCI and MRCC methods, we used a

Table 1 Mapping of $D_{\infty h}$ states to D_{2h}

$X^1\Sigma_g^+, 1^5\Sigma_g^+ \rightarrow A_g$
$1^5\Pi_u \rightarrow B_{2u} (B_{3u})$
$1^3\Sigma_u^+, 1^7\Sigma_u^+, 1^3\Delta_u, 1^1\Delta_u, 1^1\Gamma_u \rightarrow B_{1u}$
$1^1\Pi_g, 1^3\Pi_g \rightarrow B_{2g} (B_{3g})$
$1^1\Sigma_u^-, 2^1\Sigma_u^-, 1^3\Sigma_u^-, 1^3\Delta_u, 1^1\Delta_u, 1^1\Gamma_u \rightarrow A_u$

6-31G [40] [10s4p]/(3s2p) basis set and $7\Sigma_u^+$ orbitals in the calculations along the whole potential surface. The integral, SCF, and full CI calculations were carried out using MOLCAS [41] with a special interface [42]. The MO transformation left the $1\sigma_g, 2\sigma_g$ and $1\sigma_u, 2\sigma_u$ orbitals frozen leaving 6 electrons to be correlated. We considered the following states: $X^1\Sigma_g^+, 1^3\Sigma_u^+, 1^5\Sigma_g^+, 1^7\Sigma_u^+, 1^3\Pi_g, 1^5\Pi_u, 1^3\Delta_u, 1^3\Sigma_u^-, 1^1\Sigma_u^-, 1^1\Pi_g, 1^1\Gamma_u, 2^1\Sigma_u^-,$ and $1^1\Delta_u$. Their mapping onto the abelian subgroup D_{2h} of $D_{2\infty}$ is given in Table 1. Please note that the $1^1\Delta_u$ and $1^1\Gamma_u$ states show an avoided crossing at about $R = 4.44$ Bohr. As we considered only a fixed number of states at a given multiplicity the state crossing appears in Table 2 and Figs. 7, 8, 9 and 10 (the crossing states are not connected by lines).

All MRCC calculations were carried out with $S_z = 0$ wavefunctions using a CAS ($6e^-, 3\sigma_g, 1\pi_{ux}, 1\pi_{uy}, 3\sigma_u, 1\pi_{gx}, 1\pi_{gy}$) reference space. References having too few open shells for a desired target state or having almost vanishing coefficients got removed. In order to correctly select a particular state we propagated the converged MRCI wavefunctions to the MRCC amplitudes as an initial guess. We refer to [39] for further technical details.

3.2 State overlap

Exact eigenfunctions for non-degenerate eigenvalues of the Hamiltonian are orthogonal to each other. If the eigenvalues are degenerate but the eigenvectors corresponding to a specific state may be qualified with respect to additional eigenvalues of operators which commute with the Hamiltonian (good quantum numbers) the eigenvectors are still orthogonal. The non-degenerate case holds for the non-dissociative limit of N_2 while the degenerate one applies to the $N+N$ atomic limit. Therefore, all states should be orthogonal to one another at all geometries with the exception of the $\langle 2^1\Sigma_u^- | 1^1\Sigma_u^- \rangle$ state overlap at the regime of degeneracy. The $\Pi, \Delta,$ and Γ -state degeneracy does not affect orthogonality since the components of these states appear in different irreps of D_{2h} (cf. Table 1).

By construction CI methods guarantee the orthogonality of non-degenerate states naturally. Using configuration state functions (CSFs, classified by good quantum numbers) the CI vectors stay orthogonal also in case of degeneracy. Consequently, orthogonality of states is of no

Table 2 State overlaps for selected geometries

States	MRexpT		SRMRCC	
	$R = 3$ a.u.	$R = 10$ a.u.	$R = 3$ a.u.	$R = 10$ a.u.
$\langle 1^5\Sigma_g^+ X^1\Sigma_g^+ \rangle$	1.3×10^{-7}	7.9×10^{-6}	5.1×10^{-9}	4.6×10^{-1}
$\langle 1^3\Sigma_u^+ 1^1\Sigma_u^+ \rangle$	1.2×10^{-16}	2.2×10^{-18}	1.3×10^{-4}	1.2×10^{-5}
$\langle 1^3\Delta_u 1^1\Sigma_u^+ \rangle$	5.4×10^{-17}	1.6×10^{-16}	1.8×10^{-4}	7.2×10^{-5}
$\langle 1^3\Delta_u 1^3\Sigma_u^+ \rangle$	3.2×10^{-17}	2.2×10^{-14}	4.9×10^{-5}	1.5×10^{-5}
$\langle 1^7\Sigma_u^+ 1^1\Sigma_u^+ \rangle$	8.4×10^{-20}	5.2×10^{-18}	1.9×10^{-6}	1.2×10^{-5}
$\langle 1^7\Sigma_u^+ 1^3\Sigma_u^+ \rangle$	2.6×10^{-6}	6.9×10^{-6}	8.5×10^{-5}	3.2×10^{-1}
$\langle 1^7\Sigma_u^+ 1^3\Delta_u \rangle$	8.9×10^{-18}	4.4×10^{-14}	6.5×10^{-6}	5.8×10^{-5}
$\langle 1^3\Pi_g 1^1\Pi_g \rangle$	1.7×10^{-16}	1.3×10^{-16}	2.3×10^{-4}	5.4×10^{-5}
$\langle 1^1\Sigma_u^- 1^1\Sigma_u^- \rangle$	1.9×10^{-16}	9.4×10^{-15}	4.7×10^{-5}	6.4×10^{-1}
$\langle 2^1\Sigma_u^- 1^1\Sigma_u^- \rangle$	1.3×10^{-5}	2.3×10^{-3}	5.6×10^{-5}	2.5×10^{-1}
$\langle 2^1\Sigma_u^- 1^1\Sigma_u^+ \rangle$	2.3×10^{-17}	1.6×10^{-7}	1.0×10^{-4}	2.9×10^{-1}
$\langle 1^3\Delta_u 1^1\Sigma_u^- \rangle$	3.8×10^{-18}	1.7×10^{-17}	9.6×10^{-5}	3.7×10^{-6}
$\langle 1^3\Delta_u 1^1\Sigma_u^+ \rangle$	1.1×10^{-16}	3.8×10^{-16}	3.9×10^{-5}	4.0×10^{-5}
$\langle 1^3\Delta_u 2^1\Sigma_u^- \rangle$	6.1×10^{-18}	1.2×10^{-16}	4.6×10^{-5}	6.2×10^{-5}
$\langle 1^3\Sigma_u^- 1^1\Sigma_u^- \rangle$	5.0×10^{-17}	3.9×10^{-17}	3.3×10^{-4}	1.2×10^{-5}
$\langle 1^3\Sigma_u^- 1^1\Sigma_u^+ \rangle$	5.6×10^{-17}	1.8×10^{-17}	7.7×10^{-5}	7.9×10^{-6}
$\langle 1^3\Sigma_u^- 2^1\Sigma_u^- \rangle$	2.5×10^{-18}	9.0×10^{-16}	5.0×10^{-5}	1.1×10^{-5}
$\langle 1^3\Sigma_u^- 1^3\Delta_u \rangle$	1.0×10^{-16}	9.9×10^{-18}	7.0×10^{-5}	3.1×10^{-5}

$${}^a\Xi = \begin{cases} \Delta & \text{for } R = 3 \text{ Bohr} \\ \Gamma & \text{for } R = 10 \text{ Bohr} \end{cases}$$

concern with CI wavefunctions and we do not consider it in the following analysis.

For coupled cluster methods, however, the situation is different. Instead of an eigenvalue problem as for CI the solution of the coupled cluster equations involves a non-linear equation system and there is no simple rationale from linear algebra for the states to be orthogonal. The only reason for the states to be orthogonal is due to the fact that they should be approximations to eigenfunctions of the Hamiltonian. Therefore, one may interpret the state overlap as a simple measure of the quality of the wavefunction. A lack of sufficient orthogonality is expected to affect property calculations involving excited states significantly.

We calculated the state overlaps of MRexpT and SRMRCC according to

$$S_{ij} = \frac{\langle \Psi_i | \Psi_j \rangle}{\sqrt{\langle \Psi_i | \Psi_i \rangle \langle \Psi_j | \Psi_j \rangle}} \quad (10)$$

by expanding the exponential up to its natural algebraic truncation.

Table 2 shows the results for all states at two selected geometries $R = 3$ Bohr (non-degenerate case) and $R = 10$ Bohr (degenerate case) while Figs. 4 and 5 show the results for all geometries and states. We considered only those state overlaps which are not trivially zero due to their appearance in different irreps of D_{2h} according to Table 1.

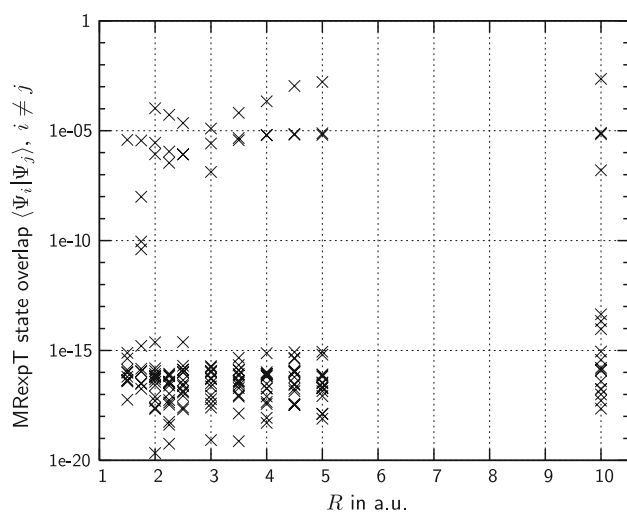


Fig. 4 State overlap error for MRexpT

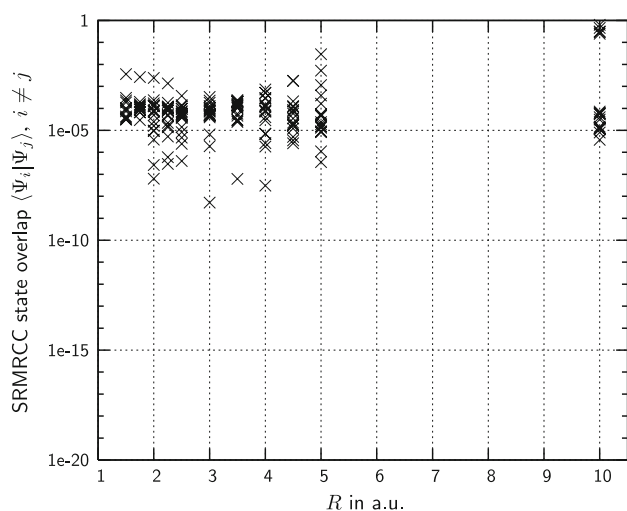


Fig. 5 State overlap error for SRMRCC

According to Table 2 and Fig. 4 the state overlaps for MRexpT may be divided into two classes: 1. overlaps which are not quite zero ($\sim 10^{-3}$ to 10^{-7} , states: $\langle 1^5\Sigma_g^+ | X^1\Sigma_g^+ \rangle$, $\langle 1^7\Sigma_u^+ | 1^3\Sigma_u^+ \rangle$, $\langle 2^1\Sigma_u^- | 1^1\Sigma_u^- \rangle$) and 2. overlaps which are actually zero ($< 10^{-14}$, remaining states). The table reveals the $\langle 2^1\Sigma_u^- | 1^1\Sigma_u^- \rangle$ overlap to be the worst with the value of 1.3×10^{-5} and 2.3×10^{-3} at the $R = 3$ and 10 Bohr geometries respectively. Since both states are of the same $D_{\infty h}$ irrep they may intermix freely at the dissociative limit and a non-vanishing overlap is reasonable. However, in the non-degenerate case they should not overlap but they still do to a certain extent. The $\langle 1^5\Sigma_g^+ | X^1\Sigma_g^+ \rangle$ and $\langle 1^7\Sigma_u^+ | 1^3\Sigma_u^+ \rangle$ are also not fully satisfactory but their overlap is somewhat smaller. Due to their different spin multiplicity the overlap does not increase as much as for the $\langle 2^1\Sigma_u^- | 1^1\Sigma_u^- \rangle$ states when approaching the degenerate case. Additionally, upon dissociation we see the

$\langle 2^1\Sigma_u^- | 1^1\Sigma_u^- \rangle$ states starting to overlap since they are both members of the A_u irrep of D_{2h} and we did not enforce the Λ_z projection.

The state overlaps for SRMRCC may be divided similarly into two classes: (1) overlaps which are not quite zero ($\sim 10^{-4}$ to 10^{-6}) and (2) overlaps which are very large. The latter show up at the dissociative limit. One should note that this problem cannot be simply addressed by the introduction of some kind of spin adaption within SRMRCC since many of the very large overlaps appear at same multiplicities [e.g. $\langle 1^1\Sigma_u^- | 1^1\Sigma_u^- \rangle$, $\langle 2^1\Sigma_u^- | 1^1\Sigma_u^- \rangle$] and spin adaption would not help. Since all states are actually converged to a residual norm less than 10^{-10} the SRMRCC wavefunction ansatz shows obviously severe difficulties to deliver proper orthogonal wavefunctions in the dissociative limit. The situation improves when going to the vicinity of the equilibrium geometry but is still not fully satisfactory. Especially in comparison to the MRexpT wavefunction SRMRCC seems to perform not reasonable in terms of state overlaps.

3.3 Spin symmetry

3.3.1 General considerations

In this subsection we shall briefly resume the implications of the spin on coupled cluster type wave functions. In the non-relativistic case it is

$$[\hat{H}, \hat{S}^2] = 0 \quad (11)$$

requiring the wavefunction to be an \hat{S}^2 eigenfunction.

There are two common ways to set up the substitution operators within the coupled cluster approach: Spin averaged ($\hat{E}_{p_1 \dots q_1 \dots, p_i, q_i}$ spatial orbitals, e.g. $\hat{E}_{p \rightarrow q} = \hat{a}_p^\dagger \hat{a}_q + \hat{a}_p^\dagger \hat{a}_{\bar{q}}$ and the bars denoting β spin, see for example [43–46]) and spin specific operators ($\hat{\tau}_{p_1 \dots q_1 \dots, p_i, q_i}$ spin orbitals, e.g. $\hat{\tau}_{p \rightarrow q} = \hat{a}_p^\dagger \hat{a}_q$, see for example [8, 37, 47, 48]). Since the spin specific operators may change the total spin (while for coupled cluster purposes they are usually chosen to conserve the S_z projection of the spin ($[\hat{S}_z, \hat{\tau}] = 0$)) they do not commute with \hat{S}^2 while the spin averaged operators do:

$$[\hat{S}^2, \hat{E}] = 0 \quad (12)$$

$$[\hat{S}^2, \hat{\tau}] \neq 0. \quad (13)$$

Naturally one might be in favor of using spin averaged operators in coupled cluster type expansions but unfortunately the \hat{E} operators with non-overlapping creator and annihilator orbital sets do not span the spin space when applied to open shell reference states. This may be healed by overlapping creator and annihilator sets but only at the price of a non-commuting algebra. The latter problem may

be cured by the use of normal ordering. We avoided this kind of complication using a spin specific (spin orbital) substitution operator. Therefore, we have to check for the spin projection of the resulting wavefunction due to Eq. 13. Since the coupled cluster methods with an untruncated cluster operator are equivalent to full CI they finally do span the spin space and are spin adapted. However, using a truncated cluster operator (e.g. singles and doubles) the latter properties will be met only approximately.

In order to analyze the spin projections of the coupled cluster approaches we consider their wavefunctions expanded in terms of determinants $|i\rangle$

$$|\Psi_{\text{det}}\rangle = \sum_i c_i |i\rangle. \quad (14)$$

For the following we impose $\langle \Psi_{\text{det}} | \Psi_{\text{det}} \rangle = 1$ and introduce a projector onto a CSF basis according to

$$\hat{P}_{\text{CSF}}^{S,S_z} = \sum_{i'} |i'\rangle \langle i'| \quad (15)$$

with $|i'\rangle$ a CSF according to

$$|i'\rangle = \xi_{\eta'} \hat{A} |\eta_{i'}\rangle |S, S_z, \nu_{i'}\rangle \quad (16)$$

with η a configuration (spatial orbital occupation pattern), \hat{A} the antisymmetrizer, ξ_{η} a normalization constant, $|S, S_z, \nu\rangle$ a spin eigenfunction with total spin S , z projection S_z and degeneracy index ν . ξ_{η} and the valid values for ν depend on the number of open shells and the total spin S [49, 50].

As described previously all calculations were carried out with $S_z = 0$ wavefunctions. Applying $\hat{P}_{\text{CSF}}^{S,S_z}$ to Eq. 14 with the desired S and $S_z = 0$ we get $|\Psi_{\text{det}}^{S,S_z}\rangle = \hat{P}_{\text{CSF}}^{S,S_z} |\Psi_{\text{det}}\rangle$. If $|\Psi_{\text{Det}}\rangle$ was a spin eigenfunction we got $\langle \Psi_{\text{det}}^{S,S_z} | \Psi_{\text{det}}^{S,S_z} \rangle = 1$. Therefore, the deviation of

$$\varepsilon := \sqrt{1 - \langle \Psi_{\text{det}}^{S,S_z} | \Psi_{\text{det}}^{S,S_z} \rangle} \quad (17)$$

from zero is a measure for the wavefunction $|\Psi_{\text{Det}}\rangle$ to contain total spin components different from the desired S . One should note that this test is stronger than the evaluation of the \hat{S}^2 expectation value. That is $\varepsilon = 0 \Leftrightarrow |\Psi_{\text{Det}}\rangle$ is a spin eigenfunction" while $\langle \Psi_{\text{Det}} | \hat{S}^2 | \Psi_{\text{Det}} \rangle = S(S+1)$ does not imply $|\Psi_{\text{Det}}\rangle$ to be an eigenfunction of \hat{S}^2 [51, 52].

Since both MRexpT and SRMRCC become exact for the untruncated cluster operator their spin projection errors at the truncated level (e.g. SD) may be considered as a measure for the quality of the wavefunction.

3.3.2 Results

In the following we report on the spin projection errors ε for SOMRCI, MRexpT and SRMRCC at reference and full wavefunction level. Projecting the SOMRCI and MRexpT wavefunctions onto the reference space the spin projection

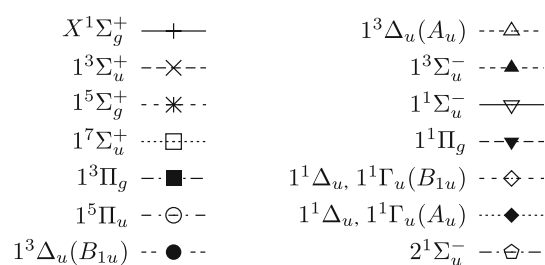


Fig. 6 N₂: legend of state symbols

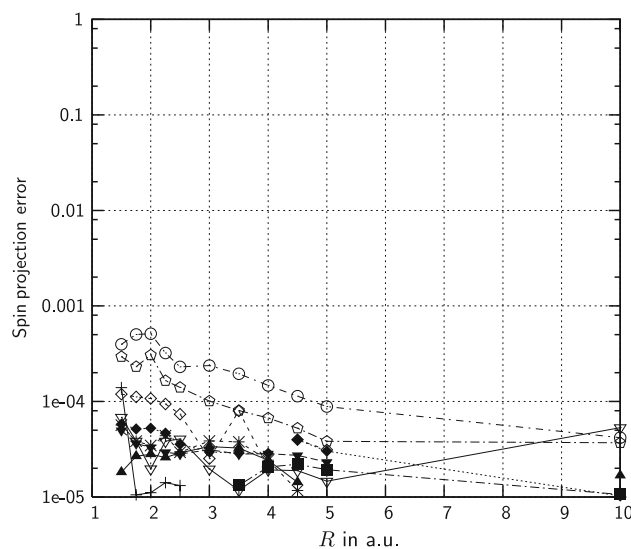


Fig. 7 Spin projection errors ε of spin orbital based MRCI, R in a.u.

errors vanish since the reference space is made by a CAS and is spin complete. In contrast to that the SRMRCC approach is possibly spin contaminated at the reference level already. Therefore we decided to investigate the following spin projection errors in detail:

- (i) SOMRCI (Fig. 7)
- (ii) MRexpT (Fig. 8)
- (iii) SRMRCC
 - (a) at reference level (Fig. 9)
 - (b) at full exponential level (Fig. 10).

The figures show the spin projection errors ε in a logarithmic plot. Figure 6 contains the state legend.

(i) Figure 7 shows the results for the spin projection errors of SOMRCI. The smallest errors are zero, the largest 5.1×10^{-4} (at $R = 2$ Bohr, $^5\Pi_u$). The spin orbital based implementation of SOMRCI leaves the spin space incomplete resulting in minor spin projection errors. While this error could be easily fixed in the case of CI by the use of a CSF expansion of the substituted determinants there is no simple fix for the coupled cluster methods when using the spin specific substitution operators $\hat{\tau}$.

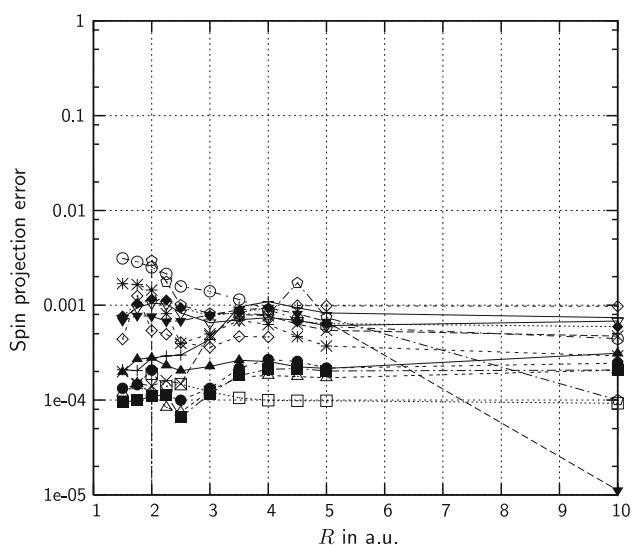


Fig. 8 MRexpT spin projection errors within full exponential space

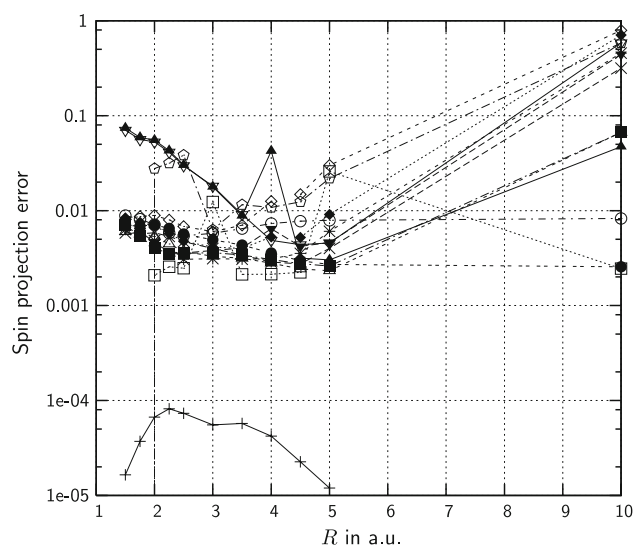


Fig. 10 SRMRCC spin projection errors ε within full exponential space

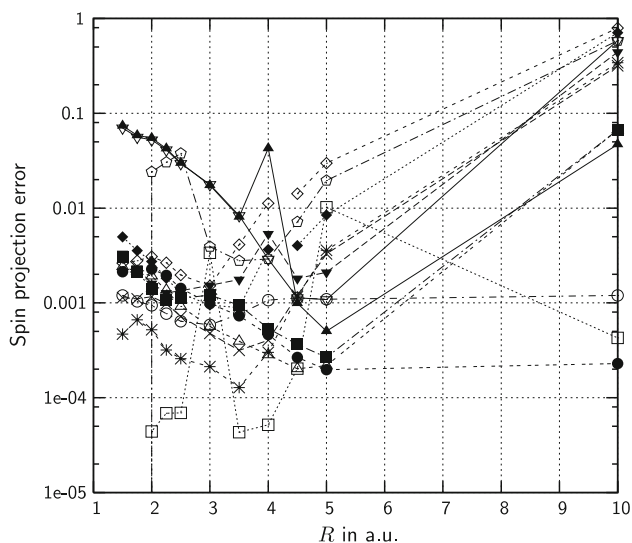


Fig. 9 SRMRCC spin projection errors within the reference space

(ii) The MRexpT spin projection errors are given in Fig. 8. In contrast to SOMRCI the errors are larger by roughly one order of magnitude. The smallest error is 6.6×10^{-5} (at $R = 2.5$ Bohr, $^3\Pi_g$), the largest 3.1×10^{-3} (at $R = 1.5$ Bohr, $^5\Pi_u$). Overall the errors behave rather continuous with no outstanding characteristic. Due to convergence difficulties with the MRexpT non-linear equation system in case of degeneracies we introduced a CSF based expansion of the reference space. We would like to point out that for non-degenerate cases MRexpT naturally delivers very small spin projection errors regardless of a CSF or determinantal expansion of the reference space. The CSF expansion within the reference space has been introduced only due to convergence difficulties for MRexpT in the case of degeneracy. All projections for $R \leq 5.0$ Bohr have been

checked to be virtually the same if performed with a determinantal reference space expansion. However, due to degeneracy effects at $R = 10$ Bohr we get partially poor spin projection errors and partially severe convergence problems of the non-linear equation system of MRexpT in case we leave the reference space CSF expansion abandoned.

(iii. a) Figure 9 shows the results for the spin projection errors of SRMRCC within the reference space. While the $X^1\Sigma_g^+$ ground state shows no spin contamination all other states show significant errors. The errors typically become largest when approaching the dissociation limit of $R = 10$ Bohr. The smallest error is zero for the $X^1\Sigma_g^+$ ground state while the largest error becomes 0.79 (at $R = 10$ Bohr, B_{1u} component of the $^1\Delta_u$ state). Interestingly, for the latter case the error gets larger than 50% meaning that the dominant multiplicity of the calculated state is different from the desired one. Analyzing the individual spin projection components yields for the singlet component $\langle \Psi_{\text{det}}^{0,0} | \Psi_{\text{det}}^{0,0} \rangle = 0.369$ and for the triplet component $\langle \Psi_{\text{det}}^{1,0} | \Psi_{\text{det}}^{1,0} \rangle = 0.631$ with higher multiplicities negligible. This is a remarkable result as we start from a (singlet) MRCI wavefunction which is propagated as an initial guess to the SRMRCC wavefunction. Consequently, the at that stage unconverged SRMRCC wavefunction is still nearly a spin eigenfunction (apart from projections outside of the MRCI space). However, upon the solution of the non-linear equation system the wavefunction changes and prefers the triplet state.

(iii. b) Finally Fig. 10 shows the results for the SRMRCC approach within the full exponential space. First of all we note the $X^1\Sigma_g^+$ state to be slightly more spin contaminated than at the reference level. Secondly we observe a significant similarity of the error within the full

exponential space and the reference space. Actually, after having analyzed the errors within the reference space already these errors are expected to propagate to the full exponential wavefunction as the reference space should be the dominating part of the wavefunction. In other words: The exponential wavefunction has no chance to recover from the spin contamination within the reference space. Actually, as can be seen from Fig. 10, it gets slightly worse, except for the $X^1\Sigma_g^+$ state at $R = 10$ Bohr. Comparing the MRexpT spin projection errors with those of SRMRCC we find the latter to be roughly one order of magnitude worse in the non-dissociative region. At the dissociative limit the spin projection errors of SRMRCC become very large.

3.3.3 Spin projection by multiplicities

Besides the analysis of the spin projection errors ε the CSF projection technique allows us to check for the “undesired” total spin components in the wavefunction explicitly. The results of the application of $\hat{P}_{\text{CSF}}^{S,S_z}$ to Eq. 14 with $M = \{1, 3, 5, 7\}$, $M = (2S + 1)$ is shown in Tables 3 and 4 exemplarily for the $^1\Sigma_u^-$ and $^3\Sigma_u^-$ states, respectively.

The tables show the weights $c^2 = \langle \Psi_{\text{det}}^{S,S_z} | \Psi_{\text{det}}^{S,S_z} \rangle$ with $S_z = 0$ and S determined by the multiplicities given in the second row of the headings of Tables 3 and 4. Naturally, the weights over all multiplicities sum up to one. Due to rounding effects at the precision given in the tables this may not always seem to be the case.

In Table 3 we see the singlet projection to be dominating as it ought to be for a $^1\Sigma_u^-$ state. However, the state is not fully pure. Interestingly, MRexpT shows no triplet and septet projection components in the wavefunction and

Table 4 MRexpT and SRMRCC spin projection by multiplicities for $^3\Sigma_u^-$, R in a.u.

R	c^2 , MRexpT				c^2 , SRMRCC			
	1 ^a	3 ^a	5 ^a	7 ^a	1 ^a	3 ^a	5 ^a	7 ^a
1.5	0	~1	0	3.9^{-8}	5.5^{-3}	9.9^{-1}	1.3^{-5}	3.8^{-8}
1.75	0	~1	0	7.3^{-8}	3.5^{-3}	~1	1.2^{-5}	6.4^{-8}
2	0	~1	0	7.8^{-8}	3.0^{-3}	~1	9.8^{-6}	8.3^{-8}
2.25	0	~1	0	5.4^{-8}	1.8^{-3}	~1	6.9^{-6}	7.3^{-8}
2.5	0	~1	0	4.1^{-8}	9.0^{-4}	~1	4.8^{-6}	5.9^{-8}
3	0	~1	0	5.1^{-8}	3.1^{-4}	~1	3.3^{-6}	5.0^{-8}
3.5	0	~1	0	6.9^{-8}	7.5^{-5}	~1	2.6^{-6}	5.1^{-8}
4	0	~1	0	6.5^{-8}	1.6^{-5}	~1	1.8^{-3}	5.4^{-8}
4.5	0	~1	0	5.0^{-8}	7.7^{-6}	~1	2.3^{-6}	5.9^{-8}
5	0	~1	0	4.6^{-8}	6.3^{-6}	~1	2.8^{-6}	8.4^{-8}
10	0	~1	0	9.7^{-8}	7.2^{-6}	~1	2.2^{-3}	1.5^{-7}

^a $M = 2S + 1$, multiplicity projection $\langle \Psi_{\text{det}}^{S,S_z} | \Psi_{\text{det}}^{S,S_z} \rangle$

the erroneous quintet projection remains nearly constant over all geometries. This is different for the SRMRCC wavefunction. It contains components of all multiplicities over the whole potential surface with the triplet component dominating (after the singlet). The latter weight error becomes 34% at $R = 10$ Bohr.

In Table 4 the triplet projection dominates as expected for the $^3\Sigma_u^-$ state. Similarly to the previous case the MRexpT wavefunction contains only two spin projection components with the erroneous septet projection being small and virtually constant over all geometries. As before the SRMRCC wavefunction contains components from all spin projections with maximum weight errors of 0.5% singlet at $R = 1.5$ Bohr and 0.2% quintet at $R = 10$ Bohr.

Table 3 MRexpT and SRMRCC spin projection by multiplicities for $^1\Sigma_u^-$, R in a.u. (due to space limitations figures a^{-b} are to be interpreted as $a \times 10^{-b}$)

R	c^2 , MRexpT				c^2 , SRMRCC			
	1 ^a	3 ^a	5 ^a	7 ^a	1 ^a	3 ^a	5 ^a	7 ^a
1.5	~1	0	5.3^{-7}	0	~1	4.9^{-3}	4.4^{-7}	2.3^{-9}
1.75	~1	0	9.0^{-7}	0	~1	3.2^{-3}	4.7^{-7}	2.1^{-9}
2	~1	0	1.1^{-6}	0	~1	2.8^{-3}	6.0^{-7}	1.9^{-9}
2.25	~1	0	1.1^{-6}	0	~1	1.7^{-3}	6.0^{-7}	9.9^{-10}
2.5	~1	0	6.9^{-7}	0	~1	8.9^{-4}	4.5^{-7}	5.9^{-10}
3	~1	0	4.3^{-7}	0	~1	3.3^{-4}	2.8^{-7}	4.2^{-10}
3.5	~1	0	4.9^{-7}	0	~1	8.3^{-5}	2.0^{-7}	6.9^{-10}
4	~1	0	5.5^{-7}	0	~1	2.4^{-5}	1.5^{-7}	2.4^{-9}
4.5	~1	0	4.8^{-7}	0	~1	1.9^{-5}	1.1^{-7}	5.7^{-9}
5	~1	0	3.7^{-7}	0	~1	2.1^{-5}	7.8^{-8}	9.0^{-9}
10	~1	0	4.6^{-7}	0	6.6^{-1}	3.4^{-1}	6.2^{-7}	1.1^{-8}

^a $M = 2S + 1$, multiplicity projection $\langle \Psi_{\text{det}}^{S,S_z} | \Psi_{\text{det}}^{S,S_z} \rangle$

4 Conclusion

After the presentation of the concepts of MRCI, MRexpT, and SRMRCC wavefunctions we discussed MRCC specific difficulties. We reported state overlap and spin projection errors of 12 low lying states of N_2 with multi-reference coupled cluster approaches.

MRexpT performs satisfactorily while SRMRCC shows significant errors due to its lack of Fermi vacuum invariance. The properties analyzed in this paper are more sensitive to symmetry issues in the wavefunction than the usually studied energetic properties. The state overlap errors of SRMRCC seem to be a serious issue. It is expected to affect property calculations of excited states (e.g. transition moments) significantly. The impact on indirect excited state calculations (e.g. linear response or EOM like approaches) on top of an SRMRCC ground state calculation is not obvious and should be investigated.

Together with the previous study on correlation energy errors of the N_2 dissociation [39] we conclude that the SRMRCC energy is usually (apart from its ambiguity and possible discontinuity) rather accurate while the associated wavefunction shows significant difficulties. For MRexpT these issues are less severe.

Analogous calculations on N_2 , e.g. for SUMRCC, MkMRCC, and BWMRCC would be very interesting.

Acknowledgments Support by the Deutsche Forschungsgemeinschaft (grant HA 5116/1-1 and SPP 1145) is gratefully acknowledged.

References

1. Coester F (1958) Nucl Phys 7:421
2. Coester F, Kümmel H (1960) Nucl Phys 17:477
3. Roos BO, Linse P, Siegbahn P, Blomberg M (1982) Chem Phys 66:197
4. Andersson K, Malmquist P-Å, Roos BO, Sadlej AJ, Wolinsky K (1990) J Phys Chem 94:5483
5. Anderson K, Malmquist P, Roos BO (1992) J Chem Phys 96:1218
6. Mukherjee D, Moitra RK, Mukhopadhyay A (1975) Mol Phys 30:1861
7. Mukherjee D (1977) Mol Phys 33:955
8. Lindgren I (1978) Int J Quantum Chem Symp 12:33
9. Lindgren I, Mukherjee D (1987) Phys Reports 151:93
10. Mukherjee D, Pal S (1989) Adv Quantum Chem 20:291
11. Jeziorski B, Monkhorst HJ (1981) Phys Rev A 24:1668
12. Paldus J, Li X (1999) Adv Chem Phys 110:1
13. Jeziorski B, Paldus J (1989) J Chem Phys 90:2714
14. Evangelista FA, Allen WD, Schaefer HF III (2006) J Chem Phys 125:154113
15. Evangelista FA, Allen WD, Schaefer HF III (2007) J Chem Phys 127:024102
16. Oliphant N, Adamowicz L (1991) J Chem Phys 94:1229
17. Li X, Paldus J (1997) J Chem Phys 107:6257
18. Li X, Paldus J (2008) J Chem Phys 128:144118
19. Li X, Paldus J (2008) J Chem Phys 128:144119
20. Mahapatra US, Datta B, Mukherjee D (1998) Mol Phys 94:157
21. Mahapatra US, Datta B, Mukherjee D (1999) J Chem Phys 110:6171
22. Masik J, Hubac I, Mach P (1998) J Chem Phys 108:6571
23. Hubac I, Pittner J, Carsky P (2000) J Chem Phys 112:8779
24. Pittner J (2003) J Chem Phys 118:10876
25. Pittner J, Li X, Paldus J (2005) Mol Phys 103:2239
26. Hanrath M (2005) J Chem Phys 123:84102
27. Hanrath M (2006) Chem Phys Lett 420:426
28. Hanrath M (2008) J Chem Phys 128:154118
29. Hanrath M (2008) Mol Phys 106:1949
30. Pople JA, Binkley JS, Seeger R (1976) Int J Quantum Chem Symp 10:1
31. Bartlett RJ (1981) Ann Rev Phys Chem 32:359
32. Piecuch P, Oliphant N, Adamowicz L (1993) J Chem Phys 99:1875
33. Kowalski K, Piecuch P (2000) J Chem Phys 113:8490
34. Lyakh DI, Ivanov VV, Adamowicz L (2005) J Chem Phys 122:24108
35. Kowalski K, Piecuch P (2001) Chem Phys Lett 344:165
36. Piecuch P, Kucharski SA, Kowalski K (2001) Chem Phys Lett 344:176
37. Kallay M, Szalay PG, Surjan PR (2002) J Chem Phys 117:980
38. Hanrath M (2008) Theor Chem Acc 121:187
39. Engels-Putzka A, Hanrath M (2008) Mol Phys (submitted)
40. Hehre W, Ditchfield R, Pople J (1972) J Chem Phys 56:2257
41. Karlstrom G, Lindh R, Malmqvist P-O, Roos BO, Ryde U, Veryazov V, Widmark P-O, Cossi M, Schimmelpfennig B, Neogrady P et al (2003) Comput Mater Sci 28:222
42. Brehms V (2001) form31, Bonn University
43. Jeziorski B, Paldus J (1988) J Chem Phys 88:5673
44. Li X, Paldus J (1994) J Chem Phys 101:8812
45. Nooijen M (1996) J Chem Phys 104:2638
46. Knowles PJ, Hampel C, Werner H-J (1993) J Chem Phys 99:5219
47. Noga J, Bartlett RJ (1987) J Chem Phys 86:7041
48. Olsen J (2000) J Chem Phys 113:7140
49. Duch W, Karwowski J (1985) Comp Phys Rep 2:93
50. Duch W, Karwowski J (1982) Int J J Quantum Chem 22:783
51. Szalay PG, Gauss J (2000) J Chem Phys 112:4027
52. Heckert M, Heun O, Gauss J, Szalay PG (2006) J Chem Phys 124:124105